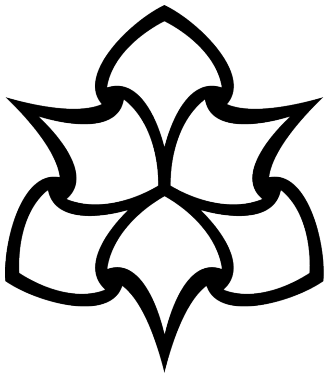

Title: NMDA receptor-dependent signalling pathways regulate arginine vasopressin expression in the paraventricular nucleus of the rat

Authors: David Lake[a], Sonia A.L. Corrêa[b,c,1] and Jürgen Müller[a,c,1]

Affiliations: [a]Warwick Medical School, University of Warwick, Coventry CV4 7AL, UK; [b]School of Life Sciences, University of Warwick, Coventry CV4 7AL, UK.; [c]School of Pharmacy and Medical Sciences, University of Bradford, Bradford BD7 1DP, UK

[1]SAL Corrêa and J Müller are Joint Senior Authors

Corresponding author: Jürgen Müller; Email: j.muller@bradford.ac.uk

Abstract

The antidiuretic hormone arginine vasopressin (AVP) regulates water homeostasis, blood pressure and a range of stress responses. It is synthesized in the hypothalamus and released from the posterior pituitary into the general circulation upon a range of stimuli. While the mechanisms leading to AVP secretion have been widely investigated, the molecular mechanisms regulating AVP gene expression are mostly unclear. Here we investigated the neurotransmitters and signal transduction pathways that activate AVP gene expression in the rat PVN using acute brain slices and quantitative real-time PCR. We show that stimulation with L-glutamate robustly induced AVP gene expression in acute hypothalamic brain slices containing the PVN. More specifically, we show that AVP transcription was stimulated by NMDA. Using pharmacological treatments, our data further reveal that the activation of ERK1/2 (PD184352), CaMKII (KN-62) and PI3K (LY294002; 740 Y-P) is involved in the NMDA-induced AVP gene expression in the PVN. Together, this study identifies NMDA-mediated cell signalling pathways that regulate AVP gene expression in the rat PVN.

Keywords

arginine vasopressin (AVP); glutamate; NMDA; gene expression; cell signalling; MAPK

1. Introduction

Arginine vasopressin (AVP) is a neurohypophysial hormone that plays a central role in the homeostatic control of osmotic balance through regulating water reabsorption by the kidneys. Dysregulation of this system leads to severe imbalances in body water. For example, in diabetes insipidus, failure to synthesise and secrete AVP into the bloodstream (central D. insipidus) or to mount an adequate response to AVP in the kidneys (nephrogenic D. insipidus) results in excessive water loss with potentially severe consequences (Robertson, 2016).

AVP is mainly synthesised in magnocellular neurons of the supraoptic and paraventricular nuclei (SON and PVN, respectively) of the hypothalamus, whose axons extend into the posterior pituitary. AVP is stored in dense-core vesicles in the axon terminals of the magnocellular neurons until released into the general circulation in response to hyperosmotic stress such as dehydration or systemic salt loading, haemorrhage, or changes in blood pressure mediated by angiotensin II (Bankir et al., 2017). AVP is also synthesized in parvocellular sections of the PVN and SON (Ueta et al., 2011). While normally inactive, AVP expression in these cells is induced by stress, which is detected through afferent inputs from different areas of the brain, including the brain stem. In contrast to magnocellular neurons, axons of parvocellular neurons project to other parts of the brain, especially the external layer of the median eminence (Papadimitriou and Priftis, 2009). AVP released from these cells activates the hypothalamic-pituitary-adrenal (HPA) axis through regulation of the hormones ACTH and CRH and regulates stress responses and social behaviour (Aguilera et al., 2008).

AVP release has been shown to be mediated by a range of stimuli, including hyperosmolality, angiotensin II, hemorrhage and other stress stimuli. For example, hyperosmolality causes activation of the osmoreceptors projecting to the SON and PVN, leading to depolarisation and phasic activity in the vasopressinergic neurons (Israel et al., 2010; Richard and Bourque, 1995). AVP release is also stimulated by angiotensin II (Glass et al., 2015) in response to low blood pressure as well as haemorrhage (Busnardo et al., 2016), which contributes to preserving the function of the cardiovascular system during this life-threatening condition. It has been shown that stimulation of AVP release in response to diverse stimuli mainly involves glutamatergic inputs (Bourque and

Richard, 2001; Busnardo et al., 2012; Israel et al., 2010; Richard and Bourque, 1995). Magnocellular neurons of the SON and PVN express both NMDA and AMPA receptors (Herman et al., 2000; Pak and Currás-Collazo, 2002). However, several studies report inconsistent roles regarding their specific contribution to inducing AVP secretion and indicate possible functional differences between the SON and PVN (Busnardo et al., 2012; Costa et al., 1992; Meeker et al., 1999).

Under conditions of increased AVP secretion, the AVP stores need to be replenished through AVP expression. However, in contrast to the mechanisms mediating AVP release, only a few studies have attempted to characterise the molecular mechanisms that regulate AVP transcription in various hypothalamic nuclei. For example, it has been shown that circadian AVP transcription in the rat suprachiasmatic nucleus (SCN) can be induced by an NMDA-mediated intracellular Ca^{2+}/calmodulin-dependent kinase IV (CaMKIV) pathway, as well as a separate vasoactive intestinal peptide (VIP) receptor subtype 2 (VPAC2)/cAMP/MAPK pathway (Rusnak et al., 2007). However, another study failed to demonstrate an increase in AVP transcription in response to treatment with glutamatergic agents in the SON in vivo, although the immediate early gene c-fos was induced under the same conditions (Kawasaki et al., 2009). There is thus a clear requirement to characterise the receptors and signalling pathways that mediate the induction of AVP gene expression in specific hypothalamic nuclei.

Here we investigated the neurotransmitters and signalling pathways that mediate activity-dependent AVP gene transcription specifically in the PVN using acute brain slices from the rat PVN. We stimulated acute rat PVN slices with glutamatergic agonists and measured the expression of AVP using qRT-PCR. We demonstrate that AVP transcription can be induced by direct glutamatergic activation of NMDA receptors (NMDARs) in the PVN. Furthermore, using pharmacological interventions, we show that the NMDAR-mediated induction of AVP transcription involves CaMKII, phosphatidylinositol-3-kinase (PI3K) and extracellular-regulated kinase 1/2 (ERK1/2). Together our results give novel insight into the molecular mechanisms that regulate AVP gene expression in the PVN of the hypothalamus, a specialised brain structure that is essential for the precise regulation of water homeostasis, blood pressure and stress responses.

2. Results

2.1 Analysis of AVP gene expression in the rat PVN using acute brain slices

To analyse AVP gene expression in the PVN, we employed an experimental paradigm using acute coronal slices from rat brain. Each slice was prepared such that it contained the PVN region of the hypothalamus (Fig 1A/B). Staining of the slices with a specific AVP antibody confirmed that the isolated region contained the PVN, including the vasopressinergic neurons (Fig 1B). In order to obtain paired samples for our analyses, the slices were divided into hemispheres and all experiments were performed using the paired 2 hemispheres from the same animal. To demonstrate that equal amounts of vasopressinergic neurons were present in each hemisphere of a given slice and that no differential gene activation took place during the preparation and culture of the slices, we measured AVP heteronuclear RNA (hnRNA) and c-fos mRNA levels in the untreated hemispheres using qRT-PCR. Importantly, AVP hnRNA was consistently detected in each hemisphere and there was no significant difference between AVP hnRNA ΔCt values for paired hemispheres of the same slice (Fig 1C/E). In addition, the immediate early gene, c-fos, was used as a marker for general neuronal activation (Kovacs, 2008; Miyata et al., 1994). Expression of c-fos mRNA was also detected consistently, and no significant difference was measured between c-fos mRNA ΔCt values for each hemisphere of a single slice (Fig 1D/E). These data demonstrate that paired PVN slices obtained from the same animal contain equal amounts of AVP hnRNA and c-fos mRNA in each hemisphere, thus confirming that both hemispheres contain similar numbers of vasopressinergic magnocellular neurons and that the neurons from both hemispheres are at a similar level of activity under basal conditions. These slices therefore represent an excellent system for the analysis of AVP gene expression in response to activation of vasopressinergic neurons of the PVN.

2.2 AVP hnRNA expression is induced by glutamatergic stimulation of the PVN

As AVP secretion is mediated by glutamatergic input into the SON and PVN (Bourque and Richard, 2001; Busnardo et al., 2012; Israel et al., 2010; Leng et al., 2001; Nissen and Renaud, 1994; Richard

and Bourque, 1995) we set out to determine whether glutamine also induces AVP gene expression. To ensure that any responses were due to the direct action of the neurotransmitters and other reagents on the vasopressinergic neurons of the VPN, the voltage-dependent Na^+ channel blocker tetrodotoxin (TTX) was used to inhibit afferent input into the neurons of the PVN. TTX application alone did not significantly affect the expression of AVP hnRNA (Fig 2A). However, we found that depolarisation of the neurons within the PVN by incubation with KCl (50 mM, 2 hours) promoted a significant increase in AVP hnRNA (Fig 2B). Importantly, direct stimulation with the neurotransmitter L-glutamate (1 mM, 2 hours) also promoted a substantial increase in AVP gene expression (Fig 2C). These data demonstrate that stimulation of AVP gene expression in the PVN is mediated by glutamatergic agonists, thus linking AVP secretion and gene expression to the same neurotransmitter.

2.3 NMDA receptors mediate the glutamatergic stimulation of AVP gene expression

Glutamate can activate a number of different receptors, including NMDA, AMPA and kainate receptors. We therefore tested the ability of the specific ionotropic glutamate receptor agonists, NMDA, AMPA and kainate (all 50 µM, 2 hours) to induce AVP hnRNA expression in hypothalamic slices containing the PVN. As above, all experiments were performed in the presence of TTX to isolate the vasopressinergic neurons from inputs that may otherwise originate from various subtypes of neurons projecting to the PVN. Importantly, only NMDA promoted a measurable increase in AVP hnRNA expression over the control samples (Fig 3A). No significant difference was seen between control and AMPA- or kainate-treated samples (Fig 3B,C). To further confirm that NMDARs are involved in the stimulation of AVP expression by glutamate, we stimulated paired slices with glutamate and pre-incubated 1 hemisphere with the specific NMDA inhibitor D-AP5 (Fig 3D). The data show a clear reduction of AVP gene expression in the presence of D-AP5, further confirmation that NMDARs mediate (at least in part) the effect of glutamate on AVP transcription. Together, these data show that AVP gene expression in the PVN is directly activated by glutamatergic stimulation of vasopressinergic neurons and that this activation is mainly mediated by NMDA receptors.

2.4 NMDA-dependent induction of AVP gene transcription in the PVN is mediated by signalling pathways encompassing CaMKII, PI3K and ERK1/2

It has been shown that activation of NMDARs results in Ca^{2+} influx, leading to activation of various Ca^{2+}-dependent protein kinases, including Ca^{2+}/calmodulin-dependent protein kinase II (CaMKII), which associates with NMDARs in postsynaptic densities (Appleby et al., 2011; Strack and Colbran, 1998). We therefore pre-incubated hypothalamic slices containing the PVN with the selective CaMKII inhibitor KN-62 (10 μM) for 1 hour, followed by stimulation of the slices with NMDA (50 μM, 2 hours) in the presence of the inhibitor. Incubation with the CaMKII inhibitor significantly abrogated the NMDA-induced increase in AVP hnRNA expression, compared to the control hemispheres without the inhibitor (Fig 4A). These data demonstrate that CaMKII is required for the transduction of the signal emanating from the NMDAR to induce AVP gene expression.

NMDA-induced CaMKII activity has been shown to activate phosphatidylinositol-3-kinase (PI3K) in the brain (Appleby et al., 2011; Wang et al., 2007). We therefore tested whether PI3K was also required for the NMDAR-mediated increase in AVP gene transcription in the hypothalamus by pre-incubating the slices with the selective PI3K inhibitor, LY294002 (10 μM), for 1 hour prior to stimulation with NMDA. LY294002 treatment significantly abrogated the NMDA-induced increase in AVP hnRNA expression in the PVN compared to the control hemisphere receiving only NMDA and no inhibitor (Fig 4B). To confirm this result, we incubated hypothalamic slices with the cell-permeable phosphopeptide activator of PI3K, 740 Y-P (Derossi et al., 1998; Williams and Doherty, 1999) (10 μg/ml, 2 hours), in the absence of NMDA. Activation of PI3K by this approach clearly promoted an increase in AVP hnRNA expression (Fig 4C), further demonstrating that PI3K is part of the signalling pathway(s) activating AVP gene expression in the PVN.

The ERK1/2 mitogen-activated protein kinase (MAPK) pathway has been shown to be activated in response to NMDAR stimulation in various brain regions (Wang et al., 2007). We

therefore incubated hypothalamic slices containing the PVN with or without the selective MEK1/2 inhibitor, PD184352 (2 μM, 1 hour) and treated both hemispheres with NMDA. Treatment with the MEK1/2 inhibitor significantly abrogated the NMDA-induced increase in AVP hnRNA expression (Fig 4D), demonstrating that the ERK1/2 MAPK pathway is involved in the induction of AVP gene expression in the PVN. Together, our data demonstrate that the NMDAR-mediated increase in AVP expression in the PVN is modified by CaMKII, PI3K and the ERK1/2 signalling pathway.

2.5 The PI3K and ERK1/2 MAPK signalling pathways contribute independently to hypothalamic AVP gene expression

Our data demonstrate that the CaMKII, PI3K and ERK1/2 MAPK signalling pathways all contribute to the activation of AVP gene expression. A link has previously been observed between the PI3K and the ERK1/2 pathways, whereby the PI3K effector Akt activates Ras (Wang et al., 2007), placing PI3K upstream of the ERK1/2 signalling module. However, it is also possible that both pathways act in parallel (Lake et al., 2016). Therefore, we investigated whether NMDAR-mediated AVP gene expression in the PVN was dependent upon the activation of the ERK1/2 pathway by upstream PI3K-mediated signalling. To do this, we activated AVP hnRNA expression using the PI3K activator, 740 Y-P and tested the ability of MEK1/2 inhibition to abrogate the stimulatory effect of 740 Y-P. However, PD184352 failed to affect AVP hnRNA expression induced by 740 Y-P (Fig 5A), suggesting that NMDAR-mediated AVP gene expression in the PVN may indeed involve separate pathways dependent on PI3K and ERK1/2, respectively. In this case, it would be expected that blocking both pathways would have a greater inhibitory effect on AVP gene expression induced by NMDA than blocking only one pathway. We tested this hypothesis by using paired hypothalamic PVN slices (hemispheres) treated with NMDA plus the PI3K inhibitor LY294002 that were further treated with or without the MEK1/2 inhibitor PD184352. Interestingly, in NMDA-stimulated slices treated with both LY294002 and PD184352, the amount of AVP hnRNA expressed in response to NMDA stimulation was significantly lower than in slices treated with LY294002 alone (Fig 5B), demonstrating that the ERK1/2 MAPK pathway contributes to AVP gene expression independently of

PI3K/AKT activation. This result confirmed that the NMDAR-mediated induction of AVP gene expression involves separate PI3K- and ERK1/2-dependent components that both contribute to the full AVP transcriptional response.

3. Discussion

In this study we have used acute rat brain slices to investigate the neurotransmitters and cellular signalling pathways that regulate AVP transcription in the PVN of the hypothalamus. This experimental system allowed us to directly stimulate the AVP-expressing neurons with neurotransmitters and specific inhibitors or activators and measure the resulting changes in AVP gene expression by quantitative RT-PCR. Using acute slices also enabled us to block the afferent inputs from a range of other neurons with TTX to ensure that the changes observed in our experiments are due to the direct effect of the added reagents on the PVN. Using this experimental paradigm, we demonstrated that direct glutamatergic stimulation of vasopressinergic neurons results in increased AVP transcription in acute rat PVN slices. Furthermore, we show that AVP transcription in the PVN is induced by activation of NMDARs and that this response is mediated by CaMKII, PI3K and the ERK1/2 MAPK pathway.

3.1 AVP gene expression in the PVN is driven by NMDAR-mediated signalling pathways

Our data show that AVP gene expression in the PVN is induced by glutamatergic input. In particular, we demonstrate that this is mediated by the activation of NMDA receptors. This observation is in line with reports showing that magnocellular neurons in the PVN preferentially express NMDARs (Herman et al., 2000) and that stimulation of rat hypothalamic explants with NMDA significantly stimulates AVP release (Costa et al., 1992). In addition, it has been reported that NMDA efficiently promotes AVP release in “punch” cultures from the rat SON containing mainly magnocellular neurons (Meeker et al., 1999), with AMPA and kainite having a significant, but smaller effect. This

observation is mirrored by our finding that NMDA initiates a significant increase in AVP gene transcription, whereas AMPA and kainite produced only a small, statistically not significant, increase.

One of the principal characteristics of NMDARs is that their activation and deactivation kinetics are much slower than those of the other ionotropic glutamate receptors (Dingledine et al., 1999). The vasopressinergic neurons would therefore require a more sustained afferent input to activate AVP gene expression. As magnocellular neurons usually store relatively large quantities of AVP in their distant processes (in the pituitary), they will only be depleted after extended periods of secretion. The potential dependence of AVP transcription on prolonged stimulation would therefore be ideal to mediate the replenishment of AVP stores in response to sustained changes in osmolality. In addition, the slow deactivation kinetics of NMDARs will allow the magnocellular neurons to fully replenish the stores before the pathway is inactivated.

Another important feature of NMDA receptors is that they are permeable for the influx of Ca^{2+}. Intracellular Ca^{2+} can activate various Ca^{2+}-dependent molecules to initiate signalling pathways leading to changes in gene expression (Rao and Finkbeiner, 2007). CaM kinases are known to associate with NMDARs in postsynaptic densities in a manner dependent on NMDAR-mediated Ca^{2+} influx (Strack and Colbran, 1998). In addition, NMDAR-dependent Ca^{2+} influx has been shown to couple to CaMKII activation in various brain tissues (Appleby et al., 2011; El Gaamouch et al., 2012; Sanhueza et al., 2011; Wang et al., 2004). Here we show that NMDAR-mediated AVP gene expression in the rat PVN is dependent on CaMKII, further implicating the NMDAR/Ca^{2+}/CaMKII signalling pathway in AVP transcription. NMDARs have also been reported to activate PI3K and thus AKT, both through Ca^{2+} influx and the activation of CaMKII (Wang et al., 2007). Importantly, we show in this study that NMDAR-mediated AVP gene expression in the rat PVN is also stimulated by PI3K.

Our data further demonstrate that the ERK1/2 MAPK pathway contributes to the induction of AVP transcription in the PVN. Using specific inhibitors in acute rat slice cultures of the PVN, we demonstrate that NMDAR-mediated AVP gene expression is directly dependent on ERK1/2 activation

in the rat PVN. This is the first direct demonstration of the requirement for ERK1/2 in mediating AVP gene expression in magnocellular neurons of hypothalamic nuclei using acute rat PVN slices.

Interestingly, the ERK1/2 MAPK pathway has been previously linked to the regulation of AVP transcription in other hypothalamic nuclei (Nikitina et al., 2014; Rusnak et al., 2007) and MAPKs regulate many important aspects of brain function, including learning and memory (Canal et al., 2011; Wang and Peng, 2016). The ERK1/2 pathway can activate various transcription factors that engage the AVP gene promoter (Greenwood et al., 2014; Iwasaki et al., 1997; Luckman et al., 1996; Yoshida et al., 2006). For example, ERK1/2 may induce the expression of c-fos, which can then bind to activator protein 1 (AP1) sites in the AVP promoter to stimulate transcription (Luckman et al., 1996; Yoshida et al., 2006). ERK1/2 may also phosphorylate the cyclic AMP response element-binding protein (CREB), which can bind to the AVP promoter at cyclic AMP response element (CRE) sites (Iwasaki et al., 1997). Indeed, the activation of ERK1/2, as well as the transcription factors CREB and Elk1, was observed in the SON of dehydrated rats (Nikitina et al., 2014). This suggested that ERK1/2-mediated CREB/Elk1 activation may be involved in the induction of AVP transcription. Finally, ERK1/2 activation may induce expression and/or activity of CREB3-like protein 1 (CREB3L1), which can bind to the AVP promoter G-box and CRE2 sequences (Greenwood et al., 2014). The relative contribution of these and other possible transcriptional regulators to AVP gene induction needs to be further investigated and may depend on the duration of the hyperosmotic stimulus (Greenwood et al., 2014).

It has been reported that PI3K can contribute to NMDAR-mediated activation of the ERK1/2 pathway, although the mechanism for this is unknown (Wang et al., 2007). This raises the possibility that PI3K activation may also lead to ERK1/2 activation and thus AVP gene expression in the PVN. However, we found that the AVP transcriptional response induced by direct activation of PI3K (using a phosphopeptide activator) was insensitive to inhibition of MEK1/2. Moreover, we show that co-inhibition of both PI3K and MEK1/2 resulted in a greater reduction in AVP expression in response to NMDA stimulation than inhibition of PI3K alone. Together, these experiments demonstrate that induction of AVP transcription by PI3K and ERK1/2 is independent of each other in the rat PVN.

Nevertheless, the mechanisms by which NMDAR stimulation mediates the activation of the ERK1/2 MAPK pathway have not been fully elucidated. However, previous reports suggested that this may involve the direct binding of NMDAR subunits to Ras guanine nucleotide releasing factors (RasGRFs), leading to activation of Ras and initiation of the Raf/MEK/ERK cascade (Wang et al., 2007). Thus, activation of NMDARs on magnocellular neurons in the PVN initiates several call signalling pathways that contribute to the induction of AVP gene expression.

In addition to the PVN, other nuclei such as the SON and SCN also produce AVP. It would be interesting to investigate whether the mechanisms regulation AVP gene expression are similar or distinct in these hypothalamic nuclei. There are very few studies that directly compare gene expression in these different nuclei. For example, one study (Ueta et al., 2011) using eGFP-expressing transgenic animals has shown that the AVP gene is induced by osmotic challenges in the PVN and SON, but not the SCN. This is in line with the function of the SCN to regulate AVP secretion diurnally. Other studies investigating the secretion of AVP have also tried to shed some light on this question, although sometimes with conflicting results. For example, previous reports used acute hypothalamic explants comprising magnocellular neurons of the SON with their axonal projections through the median eminence terminating in the neural lobe, which also included the relevant CVOs (Morsette et al., 2001; Swenson et al., 1998). These studies suggested that AVP release in the SON can be induced by activation of either NMDARs or other glutamatergic receptors (Morsette et al., 2001; Swenson et al., 1998). However, since the explants used in these studies included the CVOs, co-activation of these organs by bath application of excitatory glutamate receptor agonists may have affected the response of magnocellular AVP neurons. For this reason, we have included TTX in all experiments to block input from any other neurons into the PVN. In addition, the regulation of AVP gene expression is likely (at least partly) distinct from its secretion, as described above. It would be interesting to perform more detailed comparative studies directly comparing AVP expression in the SON and PVN under conditions that block the input form afferent neurons (e.g. by using TTX). In addition, the acute PVN slices that we established contain both magno- and parvocellular neurons, both of which can synthesize AVP. The stimuli we used (glutamate and NMDA) are likely to activate both types of

neurons. In future studies, it would be interesting to differentiate between these cell types to dissect any potential differences in the regulation of gene expression.

3.3 Conclusions

Collectively, our results reveal a novel signalling pathway regulating the activity-dependent induction of AVP gene expression in the rat PVN. Our data demonstrate that glutamate binding to NMDARs on AVP neurons initiates CaMKII, PI3K- and ERK1/2-dependent signalling pathways that lead to the induction of AVP gene expression. Subsequent investigations are necessary to clarify the coupling of NMDARs to the Raf/MEK/ERK pathway, and to determine which components act downstream of PI3K in inducing AVP transcription.

4. Experimental Procedures

4.1 Reagent preparation

L-glutamate (Abcam, Cambridge, UK) was dissolved in 1 molar eq. NaOH and used at a final concentration of 1 mM. Excitatory glutamate agonists NMDA (Tocris, Bristol, UK), kainate (Tocris) and AMPA (Abcam) were dissolved in dH_2O and used at 50 µM. The MEK1/2 inhibitor PD184352 (Sigma, St. Louis, MO, USA), CaMKII inhibitor KN-62 (Cayman Chemical, Michigan, USA), PI3K inhibitor LY294002 (Tocris) and the NMDAR inhibitor D-AP5 (Tocris) were dissolved in DMSO and used at 2 µM, 10 µM, 10 µM and 50 µM, respectively. The cell-permeable phosphopeptide activator of PI3K, 740 Y-P (Tocris), was dissolved in dH_2O and used at 10 µg/ml. The Na^+ channel blocker tetrodotoxin (TTX) citrate (Abcam) was dissolved in dH_2O and used at 2.5 µM. DMSO or NaOH at the corresponding concentrations were used as vehicle for control conditions.

4.2 Immunofluorescence and confocal microscopy

Postnatal day 8 male Sprague-Dawley rats were overdosed with anaesthetic, decapitated and the brain was removed from the skull. The brain was rapidly washed in 0.1 M PBS (pH 7.4) before fixing in 4%

paraformaldehyde in PBS at 4°C for 48 h. The brain was washed in PBS and 150 µm coronal PVN slices were obtained using an Intracel Vibratome 3000 sectioning system (Intracel, UK). Free-floating slices were permeabilised and blocked in 'carrier solution' [0.4% Triton X-100, 1% BSA in HBS (HEPES-buffered saline; 25 mM HEPES, pH 7.2; 119 mM NaCl; 5 mM KCl; 2 mM $CaCl_2$; 2 mM $MgCl_2$; 30 mM glucose)] for 6 hours at RT, followed by incubation with rabbit polyclonal anti-vasopressin antibody (1:2000; AB1565, Millipore, Billerica, MA, USA) in carrier solution for 18 hours at 4°C. Slices were washed five times in PBS (10 min per wash), incubated with AlexaFluor488-conjugated goat anti-rabbit secondary antibody (1:500; Invitrogen) and DAPI (0.1 µg/ml) in carrier solution for 4 hours at RT, followed by washing as above. Slices were mounted onto gelatin-coated glass slides (Correa et al., 1998) and coverslips were mounted with Mowiol (Kuratay Europe GmbH, Frankfurt, Germany) as described (Canal et al., 2011; Eales et al., 2014). Immunofluorescent staining was observed using a 40x oil-immersion lens on a Zeiss LSM 510 Meta confocal microscope (Carl Zeiss, Oberkochen, Germany). Composite images shown in Fig 1A were generated by merging 65 individual confocal images using AutoStitch v2.2 (Ma et al., 2007).

4.3 Preparation and stimulation of acute PVN slices

Postnatal day 8-12 male Sprague-Dawley rats were overdosed with anaesthetic, decapitated and brains were rapidly removed from the skull into ice-cold artificial cerebrospinal fluid (aCSF; 124 mM NaCl, 3 mM KCl, 2 mM $CaCl_2$, 26 mM $NaHCO_3$, 1.25 mM NaH_2PO_4, 10 mM D-glucose and 1 mM $MgSO_4$, pH 7.4) bubbled with O_2. A single coronal 450 µm PVN slice (at approximately Bregma -1.72 mm; see Fig 1A,B) per animal was obtained using an Intracel Vibratome 3000 sectioning system. The slices were trimmed so that they did not contain the SON, which is located at the ventral side of the slice. All slices were then divided into left and right hemispheres by carefully cutting along the third ventricle under a dissecting microscope. All experiments were conducted using the paired hemispheres so that the samples in each specific experiment were from the same animal. Subsequent steps were performed in oxygenated aCSF at 32°C. Each hemisphere was stabilised for 1 hour, pre-incubated for 1 hour in the appropriate reagents (TTX plus inhibitors or activators) and stimulated for 2 hours with the

appropriate agonists in the presence of the pre-incubation reagents. The exact composition of the reagents in each of the samples is indicated in the figures and the legends.

4.4 RNA extraction and cDNA synthesis

At the end of the 2 hour stimulation, total RNA was isolated from slices (each weighing approximately 20 µg) by direct transfer into TRIzol reagent (Fisher Scientific, Loughborough, UK). Slices were disrupted using sterile pestles and homogenised by passage through a QIAshredder column (Qiagen, Limburg, Netherlands), followed by chloroform phase separation and purification using the PureLink RNA mini kit (Fisher Scientific). Purified RNA was subjected to on-column DNase treatment (Fisher Scientific) and the concentration and purity of the RNA was assessed spectrophotometrically using the NanoDrop ND-1000 (NanoDrop, Wilmington, DE, USA). RNA used for all further experiments had an A_{260}/A_{280} ratio of 1.9 – 2.25. First-strand cDNA synthesis was performed with 500 ng RNA using M-MLV reverse transcriptase (Invitrogen, Carlsbad, CA, USA) with 200 ng random hexamer primers (Fisher Scientific) in a total reaction volume of 20 µl, according to the manufacturer's protocol.

4.5 qRT-PCR

Primers (Table 1) for the detection of β-actin mRNA, c-fos mRNA, AVP mRNA and AVP heteronuclear RNA (hnRNA) have been published elsewhere (Kawasaki et al., 2009; Zeybel et al., 2012); GAPDH mRNA primers were designed with the help of Primer3Plus software (Untergasser et al., 2007). The levels of AVP hnRNA – rather than mRNA – were analysed here because they have been shown to acutely and reliably change in response to osmotic (Herman et al., 1991; Ponzio et al., 2007; Yue et al., 2006) and other stimuli such as acute stress (Ma et al., 1997). In contrast, AVP mRNA is abundant and relatively unaffected by short-term stimuli. Therefore, measurement of AVP hnRNA was chosen for analysing acute changes in AVP gene expression.

Reverse transcriptase PCR (RT-PCR) was performed using each set of primers as described (Shaheen et al., 2014; Wall et al., 2018) and amplification of a single correct product was checked by agarose gel electrophoresis followed by sequencing (GATC Biotech, London, UK). Primer standard curves

were performed to estimate the PCR efficiencies for each primer pair; the efficiencies of all five primer sets used in the current study were between 85 and 106%. qRT-PCR was performed using an AB 7500 Fast machine (Applied Biosystems, Life Technologies, Paisley, UK). cDNA was diluted 1:50 in dH_2O and each reaction comprised 5 µl diluted cDNA, 10 µl Precision (or PrecisionPlus) 2x real-time PCR MasterMix with SYBR green (Primerdesign, Southampton, UK) and 120 nM primers in a final volume of 20 µl. The PCR cycling conditions were as follows: 95°C for 10 min (for Precision; 2 min for PrecisionPlus), then 40 cycles of 95°C for 15 s, 60°C for 1 min, followed by melt curve recording between 60 and 95°C. Cycle threshold (Ct) values were determined by the AB 7500 Fast software and were routinely checked manually. qRT-PCR reactions were run in triplicate and corresponding samples in a given experiment were run on the same plate. An additional reaction using the AVP hnRNA primers was performed on samples that had not been treated with reverse transcripase (-RT) to check for genomic DNA (gDNA) contamination; templates routinely had Ct differences >6 for the +RT versus –RT samples, representing little if any gDNA contamination.

Table 1. Details of qRT-PCR primers used in the current study.

Primer pairs	Sequence	Product (bp)	T_A (°C)	T_M (°C)
GAPDH mRNA	5'-agttcaacggcacagtcaag (forward) 5'-gtggtgaagacgccagtaga (reverse)	148	60	82.2
β-actin mRNA	5'-agccatgtacgtagccatcc (forward) 5'-ctctcagctgtggtggtgaa (reverse)	228	60	86.2
c-fos mRNA	5'-agcatgggctcccctgtca (forward) 5'-gagaccagagtgggctgca (reverse)	134	60	84.1
AVP mRNA	5'-tgcctgctacttccagaactgc (forward) 5'-aggggagacactgtctcagctc (reverse)	77	60	80.1
AVP hnRNA	5'-gccctcacctctgcctgcta (forward) 5'-cctgaacggaccacagtggt (reverse)	100	60	82.8

T_A, annealing temperature; T_M, PCR product melting temperature.

4.6 Data analysis

AVP gene expression was measured as changes in AVP hnRNA, which has been shown to be a sensitive indicator of acute changes in AVP transcription (Herman et al., 1991; Ma et al., 1997; Ponzio et al., 2007; Yue et al., 2006). Normalisation was performed using the geometric mean of GAPDH, β-

actin and AVP mRNA as reference. AVP mRNA was included in the reference to calibrate for the number of vasopressinergic PVN neurons present within the slices, as it has been shown that AVP neurons store relatively large levels of AVP mRNA and that its levels do not significantly change upon stimulation (Ma et al., 1997; Ponzio et al., 2007; Yue et al., 2006), in contrast to that of the hnRNA. ΔCt values for c-fos mRNA and AVP hnRNA were calculated by subtracting the geometric mean of GAPDH, β-actin and AVP mRNA Ct values from the relevant c-fos mRNA or AVP hnRNA mean Ct values. Relative quantification of c-fos mRNA and AVP hnRNA changes was performed using the $2^{-\Delta\Delta Ct}$ method (Livak and Schmittgen, 2001). All treatments were performed in paired samples by using two hemispheres of the same animal's PVN slice. Statistical differences between ΔCt values of paired treatments were evaluated using a paired two-tailed t test and data were analysed and presented as percentage of the appropriate control (without 1 of the applied reagents) using GraphPad Prism 6 ($p<0.05$ was considered significant). For graphical presentation of the variances, within-subject SEMs were calculated according to the method of Cousineau et al (Cousineau, 2005). In addition, graphs representing the differences of the means, together with the relevant 95% CIs, were prepared.

4.7 Ethical approval

All applicable international, national, and/or institutional guidelines for the care and use of animals were followed. All procedures performed in studies involving animals were in accordance with the ethical standards of the institution at which the studies were conducted. This article does not contain any studies with human participants performed by any of the authors.

5. Acknowledgements

This study was supported by a generous donation from Jonathan Feuer. We are grateful for his financial support that has made this work possible. We would also like to thank Dr Mark Wall (University of Warwick) for his help with the preparation of the brain slices during the revision of the manuscript.

6. References

Aguilera, G., et al., 2008. The parvocellular vasopressinergic system and responsiveness of the hypothalamic pituitary adrenal axis during chronic stress. Prog Brain Res. 170**,** 29-39.

Appleby, V.J., et al., 2011. LTP in hippocampal neurons is associated with a CaMKII-mediated increase in GluA1 surface expression. J. Neurochem. 116**,** 530-543.

Bankir, L., Bichet, D.G., Morgenthaler, N.G., 2017. Vasopressin: physiology, assessment and osmosensation. J Intern Med. 282**,** 284-297.

Bourque, C.W., Richard, D., 2001. Axonal projections from the organum vasculosum lamina terminalis to the supraoptic nucleus: functional analysis and presynaptic modulation. Clin Exp Pharmacol Physiol. 28**,** 570-4.

Busnardo, C., et al., 2012. Ionotropic Glutamate Receptors in Hypothalamic Paraventricular and Supraoptic Nuclei Mediate Vasopressin and Oxytocin Release in Unanesthetized Rats. Endocrinol. 153**,** 2323-2331.

Busnardo, C., et al., 2016. NMDA and non-NMDA glutamate receptors in the paraventricular nucleus of the hypothalamus modulate different stages of hemorrhage-evoked cardiovascular responses in rats. Neuroscience. 320**,** 149-59.

Canal, F., et al., 2011. Compartmentalization of the MAPK scaffold protein KSR1 modulates synaptic plasticity in hippocampal neurons. The FASEB Journal. 25**,** 2362-2372.

Correa, S.A., Correa, F.M., Hoffmann, A., 1998. Stereotaxic atlas of the telencephalon of the weakly electric fish Gymnotus carapo. J Neurosci Methods. 84**,** 93-100.

Costa, A., et al., 1992. Differential effects of neuroexcitatory amino acids on corticotropin-releasing hormone-41 and vasopressin release from rat hypothalamic explants. Endocrinol. 131**,** 2595-2602.

Cousineau, D., 2005. Confidence intervals in within-subject designs: A simpler solution to Loftus and Masson's method. Tutorials in Quantitative Methods for Psychology. 1**,** 42-45.

Derossi, D., et al., 1998. Stimulation of Mitogenesis by a Cell-Permeable PI 3-Kinase Binding Peptide. Biochem. Biophys. Res. Commun. 251**,** 148-152.

Dingledine, R., et al., 1999. The glutamate receptor ion channels. Pharmacol Rev. 51**,** 7-61.

Eales, K.L., et al., 2014. The MK2/3 cascade regulates AMPAR trafficking and cognitive flexibility. Nat Commun. 5**,** 4701.

El Gaamouch, F., et al., 2012. Interaction Between αCaMKII and GluN2B Controls ERK-Dependent Plasticity. J. Neurosci. 32**,** 10767-10779.

Glass, M.J., et al., 2015. NMDA Receptor Plasticity in the Hypothalamic Paraventricular Nucleus Contributes to the Elevated Blood Pressure Produced by Angiotensin II. J Neurosci. 35**,** 9558-67.

Greenwood, M., et al., 2014. Transcription Factor CREB3L1 Regulates Vasopressin Gene Expression in the Rat Hypothalamus. J. Neurosci. 34**,** 3810-3820.

Herman, J.P., et al., 1991. In Situ Hybridization Analysis of Arginine Vasopressin Gene Transcription Using Intron-Specific Probes. Mol. Endocrinol. 5**,** 1447-1456.

Herman, J.P., et al., 2000. Expression of ionotropic glutamate receptor subunit mRNAs in the hypothalamic paraventricular nucleus of the rat. J. Comp. Neurol. 422**,** 352-362.

Israel, J.M., Poulain, D.A., Oliet, S.H., 2010. Glutamatergic inputs contribute to phasic activity in vasopressin neurons. J Neurosci. 30**,** 1221-32.

Iwasaki, Y., et al., 1997. Positive and Negative Regulation of the Rat Vasopressin Gene Promoter. Endocrinol. 138**,** 5266-5274.

Kawasaki, M., et al., 2009. Neurotransmitter regulation of c-fos and vasopressin gene expression in the rat supraoptic nucleus. Exp. Neurol. 219**,** 212-222.

Kovacs, K.J., 2008. Measurement of immediate-early gene activation- c-fos and beyond. J Neuroendocrinol. 20**,** 665-72.

Lake, D., Correa, S.A., Muller, J., 2016. Negative feedback regulation of the ERK1/2 MAPK pathway. Cell Mol Life Sci. 73**,** 4397-4413.
Leng, G., et al., 2001. Responses of Magnocellular Neurons to Osmotic Stimulation Involves Coactivation of Excitatory and Inhibitory Input: An Experimental and Theoretical Analysis. J. Neurosci. 21**,** 6967-6977.
Livak, K.J., Schmittgen, T.D., 2001. Analysis of relative gene expression data using real-time quantitative PCR and the 2(-Delta Delta C(T)) Method. Methods. 25**,** 402-8.
Luckman, S.M., Dye, S., Cox, H.J., 1996. Induction of members of the Fos/Jun family of immediate-early genes in identified hypothalamic neurons: in vivo evidence for differential regulation. Neurosci. 73**,** 473-485.
Ma, B., et al., 2007. Use of Autostitch for automatic stitching of microscope images. Micron. 38**,** 492-9.
Ma, X.M., Levy, A., Lightman, S.L., 1997. Rapid changes in heteronuclear RNA for corticotrophin-releasing hormone and arginine vasopressin in response to acute stress. J Endocrinol. 152**,** 81-9.
Meeker, R.B., et al., 1999. Functional activation of punch-cultured magnocellular neuroendocrine cells by glutamate receptor subtypes. J. Neurosci. Methods. 89**,** 57-67.
Miyata, S., Nakashima, T., Kiyohara, T., 1994. Expression of c-fos immunoreactivity in the hypothalamic magnocellular neurons during chronic osmotic stimulations. Neurosci Lett. 175**,** 63-6.
Morsette, D.J., Sidorowicz, H., Sladek, C.D., 2001. Role of non-NMDA receptors in vasopressin and oxytocin release from rat hypothalamo-neurohypophysial explants. Am. J. Physiol. Regul. Integr. Comp. Physiol. 280**,** R313-R322.
Nikitina, L., et al., 2014. Role of the ERK signaling pathway in regulating vasopressin secretion in dehydrated rats. Biotech. Histochem. 89**,** 199-208.
Nissen, R., Renaud, L.P., 1994. GABA receptor mediation of median preoptic nucleus-evoked inhibition of supraoptic neurosecretory neurones in rat. J. Physiol. 479**,** 207-216.
Pak, C.W., Currás-Collazo, M.C., 2002. Expression and plasticity of glutamate receptors in the supraoptic nucleus of the hypothalamus. Microsc. Res. Tech. 56**,** 92-100.
Papadimitriou, A., Priftis, K.N., 2009. Regulation of the hypothalamic-pituitary-adrenal axis. Neuroimmunomodulation. 16**,** 265-71.
Ponzio, T.A., Yue, C., Gainer, H., 2007. An intron-based real-time PCR method for measuring vasopressin gene transcription. J. Neurosci. Methods. 164**,** 149-154.
Rao, V.R., Finkbeiner, S., 2007. NMDA and AMPA receptors: old channels, new tricks. Trends Neurosci. 30**,** 284-291.
Richard, D., Bourque, C.W., 1995. Synaptic control of rat supraoptic neurones during osmotic stimulation of the organum vasculosum lamina terminalis in vitro. J. Physiol. 489**,** 567-577.
Robertson, G.L., 2016. Diabetes insipidus: Differential diagnosis and management. Best Pract Res Clin Endocrinol Metab. 30**,** 205-18.
Rusnak, M., et al., 2007. Depolarization and Neurotransmitter Regulation of Vasopressin Gene Expression in the Rat Suprachiasmatic Nucleus In Vitro. J. Neurosci. 27**,** 141-151.
Sanhueza, M., et al., 2011. Role of the CaMKII/NMDA Receptor Complex in the Maintenance of Synaptic Strength. J. Neurosci. 31**,** 9170-9178.
Shaheen, F., et al., 2014. Extra-nuclear telomerase reverse transcriptase (TERT) regulates glucose transport in skeletal muscle cells. Biochim Biophys Acta. 1842**,** 1762-9.
Strack, S., Colbran, R.J., 1998. Autophosphorylation-dependent Targeting of Calcium/ Calmodulin-dependent Protein Kinase II by the NR2B Subunit of theN-Methyl- d-aspartate Receptor. J. Biol. Chem. 273**,** 20689-20692.
Swenson, K.L., et al., 1998. N-Methyl-d-Aspartic Acid Stimulation of Vasopressin Release: Role in Osmotic Regulation and Modulation by Gonadal Steriods. J. Neuroendocrinol. 10**,** 679-685.
Ueta, Y., Dayanithi, G., Fujihara, H., 2011. Hypothalamic vasopressin response to stress and various physiological stimuli: visualization in transgenic animal models. Horm Behav. 59**,** 221-6.

Untergasser, A., et al., 2007. Primer3Plus, an enhanced web interface to Primer3. Nucleic Acids Res. 35**,** W71-W74.
Wall, M.J., et al., 2018. The Temporal Dynamics of Arc Expression Regulate Cognitive Flexibility. Neuron. 98**,** 1124-1132 e7.
Wang, H., Peng, R.Y., 2016. Basic roles of key molecules connected with NMDAR signaling pathway on regulating learning and memory and synaptic plasticity. Mil Med Res. 3**,** 26.
Wang, J., et al., 2004. Glutamate signaling to ras-MAPK in striatal neurons. Mol. Neurobiol. 29**,** 1-14.
Wang, J.Q., Fibuch, E.E., Mao, L., 2007. Regulation of mitogen-activated protein kinases by glutamate receptors. J. Neurochem. 100**,** 1-11.
Williams, E.-J., Doherty, P., 1999. Evidence for and against a Pivotal Role of PI 3-Kinase in a Neuronal Cell Survival Pathway. Mol. Cell. Neurosci. 13**,** 272-280.
Yoshida, M., et al., 2006. Identification of a Functional AP1 Element in the Rat Vasopressin Gene Promoter. Endocrinol. 147**,** 2850-2863.
Yue, C., et al., 2006. Studies of oxytocin and vasopressin gene expression in the rat hypothalamus using exon- and intron-specific probes. Am. J. Physiol. Regul. Integr. Comp. Physiol. 290**,** R1233-R1241.
Zeybel, M., et al., 2012. Multigenerational epigenetic adaptation of the hepatic wound-healing response. Nat. Med. 18**,** 1369-1377.

7. Figure Captions:

Fig 1. Acute rat brain slices contain equal numbers of vasopressinergic neurons in both hemispheres. (A) Diagrammatic representation of the PVN. 3V, third ventricle; V, ventral part; DC, dorsal cap; LM, lateral magnocellular part; MP, medial parvicellular part. **(B)** Immunofluorescence staining of the PVN region using a specific antibody against AVP, clearly showing the vasopressinergic neurons in both hemispheres. DAPI was used to stain the nuclei. Scale bar = 200 µm. **(C/D)** Total RNA was extracted and the expression of AVP hnRNA **(C)** and c-fos mRNA **(D)** was measured in left and right hemispheres of 450 µm acute coronal rat PVN slices by qRT-PCR. ΔΔCt values were expressed as a percentage of ΔΔCt for the left hemisphere. The data are presented as the mean ± SEM (AVP hnRNA, *n*=4; c-fos mRNA, *n*=3). No significant difference was detected for either AVP hnRNA or c-fos mRNA expression between the two hemispheres (paired two-tailed t test). **(E)** The differences between ΔCt values for paired slices were calculated and the data presented are the mean of these differences, with the error bars representing the 95% CI.

Fig 2. AVP gene expression in the rat PVN is stimulated by glutamatergic stimuli. The expression of AVP hnRNA was measured in 450 µm acute coronal rat PVN slices by qRT-PCR. Slices were dissected into left and right hemispheres, one of which was used as the paired control in each experiment. Slices were stabilised in aCSF at 32°C for 1 hour, followed by incubation with (or without) 2.5 µM TTX for 1 hour **(A)**. In **B/C**, all slices were treated for 1 hour with 2.5 µM TTX, followed by incubation with (or without) 50 mM KCl **(B)** or 1 mM L-Glutamate **(C)** for 2 hours. Total RNA was then extracted and processed for analysis by qRT-PCR. AVP hnRNA ΔΔCt values were expressed as a percentage of ΔΔCt for control slices, and the data presented are the mean ± SEM (*n*=5 per condition) [*p<0.05, ***p<0.001 (paired two-tailed t test)]. In addition, the differences between ΔCt values for paired slices were calculated and the data presented are the mean of these differences, with the error bars representing the 95% CI.

Fig 3. The glutamatergic induction of AVP gene expression in the rat PVN is facilitated by NMDARs. The expression of AVP hnRNA was measured in 450 µm acute coronal rat PVN slices by qRT-PCR. Slices were dissected into left and right hemispheres, one of which was used as the paired control in each experiment. Slices were stabilised in aCSF at 32°C for 1 hour, followed by incubation with 2.5 µM TTX for another hour. Slices were then incubated with (or without) 50 µM NMDA **(A)**, 50 µM AMPA **(B)** or 50 µM kainate **(C)** for 2 hours (in the presence of TTX). Total RNA was then extracted and processed for analysis by qRT-PCR. In **(D)** slices were incubated with (or without) D-AP5 together with TTX for 1 hour before stimulation with glutamate (in the presence of TTX plus vehicle or D-AP5) for 2 hours. AVP hnRNA ΔΔCt values were expressed as a percentage of ΔΔCt for slices in TTX alone, and the data presented are the mean ± SEM (n=3-4 per condition) [*p<0.05 versus TTX alone (A-C) or TTX/glutamine (D); paired two-tailed t test]. In addition, the differences between ΔCt values for paired slices were calculated and the data presented are the mean of these differences, with the error bars representing the 95% CI.

Fig 4. NMDAR-mediated AVP gene expression in the rat PVN is dependent on CaMKII, PI3K and ERK1/2. The expression of AVP hnRNA was measured in 450 µm acute coronal rat PVN slices by qRT-PCR. Slices were dissected into left and right hemispheres, one of which was used as the paired control in each experiment. Slices were stabilised in aCSF at 32°C for 1 hour, followed by a 1 hour incubation with 2.5 µM TTX plus either **(A)** the CaMKII inhibitor KN-62 (10 µM), **(B)** the PI3K inhibitor LY294002 (10 µM), or **(D)** the MEK1/2 inhibitor PD184352 (2 µM). Slices were then incubated with 50 µM NMDA for 2 hours (in the presence of TTX and inhibitor). In **(C)**, stabilised slices were incubated for 1 hour with 2.5 µM TTX, followed by a 2 hour incubation with 10 µg/ml 740 Y-P in the presence of TTX. For all experiments, total RNA was extracted and processed for analysis by qRT-PCR. AVP hnRNA ΔΔCt values are expressed as a percentage of ΔΔCt relative to the corresponding control. The data are presented as the mean ± SEM (n=4-5 per condition) [*p<0.05, **p<0.01 (paired two-tailed t test)]. The differences between ΔCt values for paired slices were

calculated and the data presented are the mean of these differences, with error bars representing the 95% CI.

Fig 5. NMDAR-mediated AVP gene expression in the rat PVN is dependent on both PI3K- and ERK1/2-dependent pathways. The expression of AVP hnRNA was measured in 450 μm acute coronal rat PVN slices by qRT-PCR. Slices were dissected into left and right hemispheres, one of which was used as a paired control in each experiment. Slices were stabilised in aCSF at 32°C for 1 hour. **(A)** Stabilised slices were incubated for another 1 hour in 2.5 μM TTX together with (or without) 2 μM PD184352. The slices were then incubated with 10 μg/ml 740 Y-P in the presence of TTX plus (or minus) inhibitor for a further 2 hours. **(B)** Stabilised slices were incubated for 1 hour with 2.5 μM TTX together with (or without) 2 μM PD184352, followed by a 2 hour incubation with 50 μM NMDA plus 10 μM LY294002. Total RNA was extracted from all samples and processed for analysis by qRT-PCR. ΔΔCt values are expressed as a percentage of ΔΔCt relative to the paired control slices and the data presented are the mean ± SEM (a: n=7, b: *n*=5). [**p*<0.05 (paired two-tailed t test)] The differences between ΔCt values for paired slices were calculated and the data presented are the mean, with the error bars representing the 95% CI.

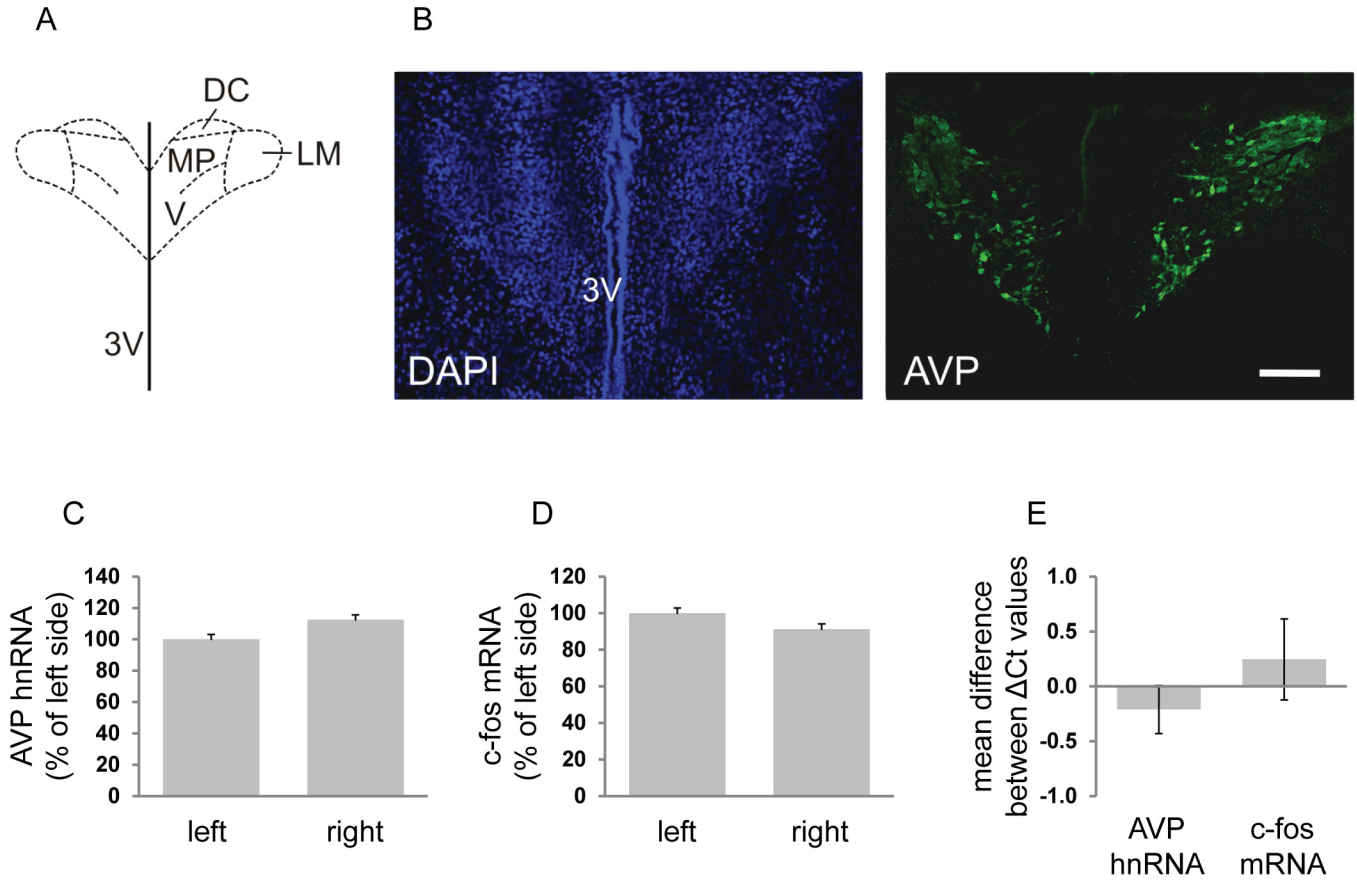
A
DC
MP
LM
V
3V
B
3V
DAPI
AVP
C
AVP hnRNA (% of left side)
140
120
100
80
60
40
20
0
left
right
D
c-fos mRNA (% of left side)
120
100
80
60
40
20
0
left
right
E
mean difference between ΔCt values
1.0
0.5
0.0
-0.5
-1.0
AVP hnRNA
c-fos mRNA

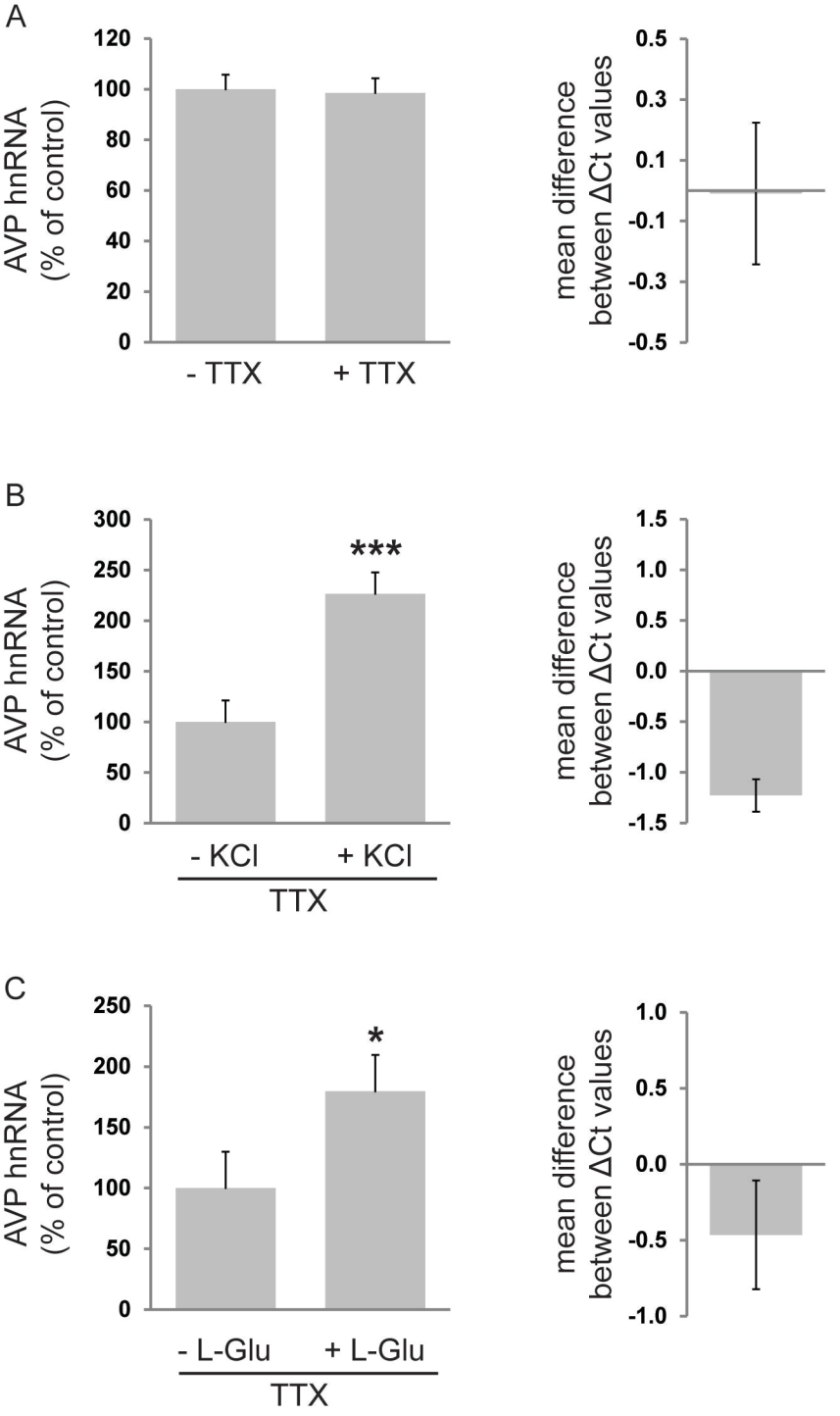
A
AVP hnRNA
(% of control)
120
100
80
60
40
20
0
- TTX
+ TTX
mean difference
between ΔCt values
0.5
0.3
0.1
-0.1
-0.3
-0.5
B
AVP hnRNA
(% of control)
300
250
200
150
100
50
0
***
- KCl
+ KCl
TTX
mean difference
between ΔCt values
1.5
1.0
0.5
0.0
-0.5
-1.0
-1.5
C
AVP hnRNA
(% of control)
250
200
150
100
50
0
*
- L-Glu
+ L-Glu
TTX
mean difference
between ΔCt values
1.0
0.5
0.0
-0.5
-1.0

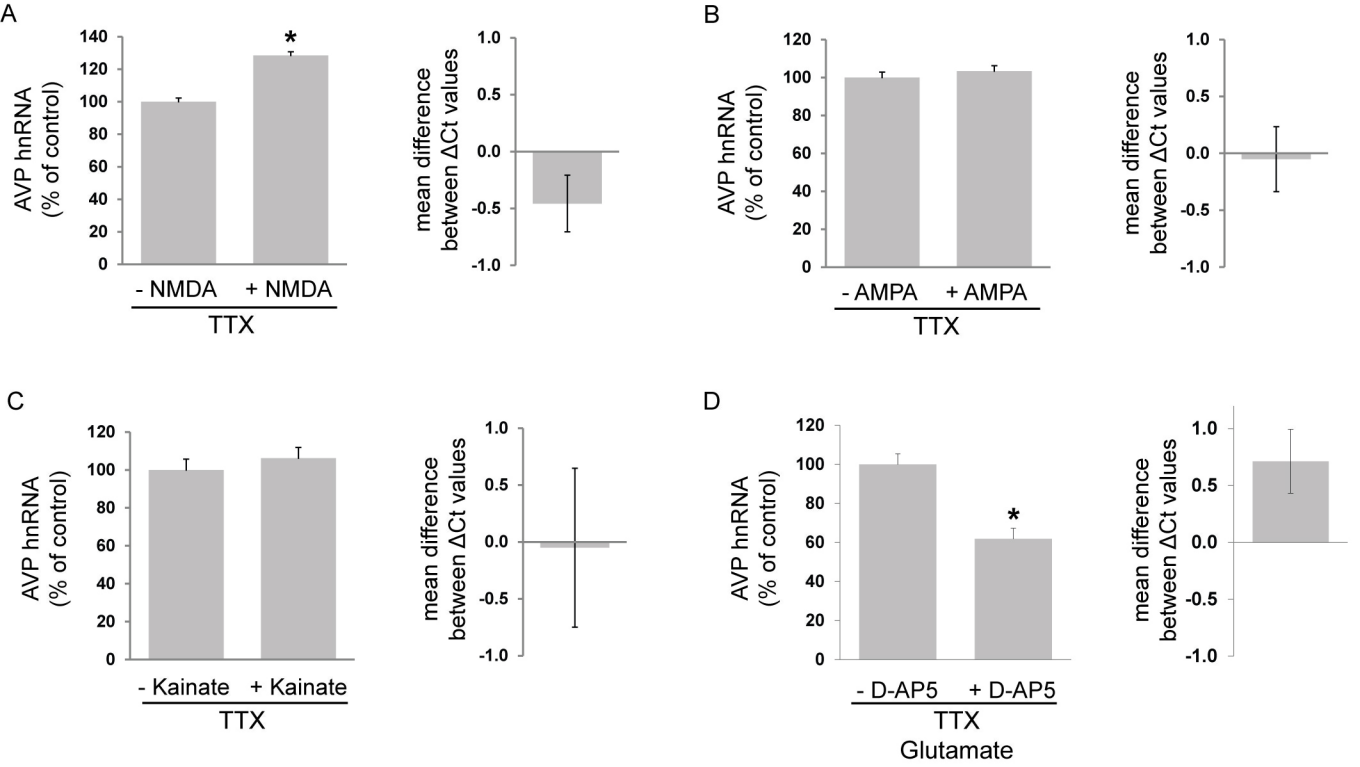
A
AVP hnRNA (% of control)
140
120
100
80
60
40
20
0
*
- NMDA
+ NMDA
TTX
mean difference between ΔCt values
1.0
0.5
0.0
-0.5
-1.0
B
AVP hnRNA (% of control)
120
100
80
60
40
20
0
- AMPA
+ AMPA
TTX
mean difference between ΔCt values
1.0
0.5
0.0
-0.5
-1.0
C
AVP hnRNA (% of control)
120
100
80
60
40
20
0
- Kainate
+ Kainate
TTX
mean difference between ΔCt values
1.0
0.5
0.0
-0.5
-1.0
D
AVP hnRNA (% of control)
120
100
80
60
40
20
0
*
- D-AP5
+ D-AP5
TTX
Glutamate
mean difference between ΔCt values
1.0
0.5
0.0
-0.5
-1.0

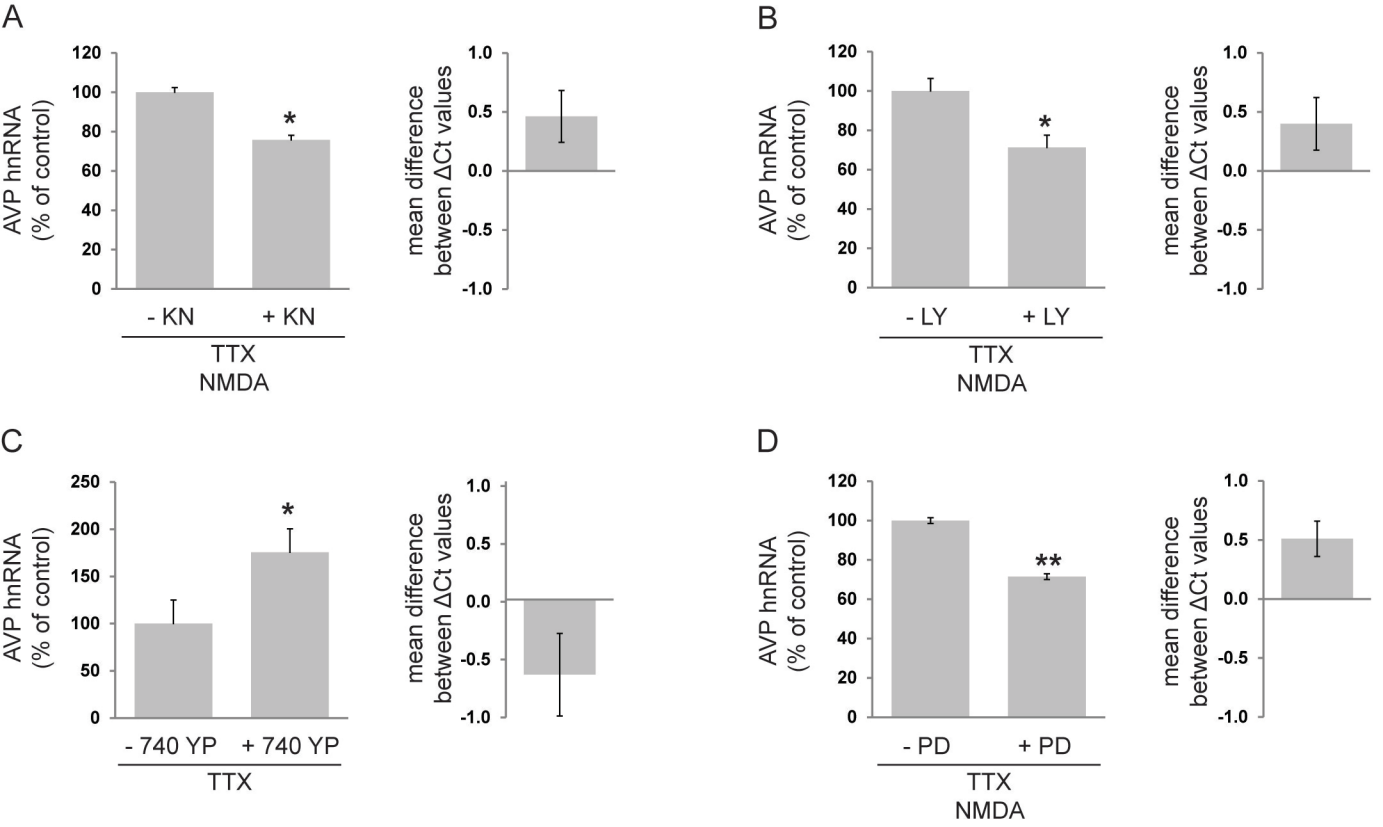
A
AVP hnRNA
(% of control)
120
100
80
60
40
20
0
*
- KN
+ KN
TTX
NMDA
mean difference
between ΔCt values
1.0
0.5
0.0
-0.5
-1.0
B
AVP hnRNA
(% of control)
120
100
80
60
40
20
0
*
- LY
+ LY
TTX
NMDA
mean difference
between ΔCt values
1.0
0.5
0.0
-0.5
-1.0
C
AVP hnRNA
(% of control)
250
200
150
100
50
0
*
- 740 YP
+ 740 YP
TTX
mean difference
between ΔCt values
1.0
0.5
0.0
-0.5
-1.0
D
AVP hnRNA
(% of control)
120
100
80
60
40
20
0
**
- PD
+ PD
TTX
NMDA
mean difference
between ΔCt values
1.0
0.5
0.0
-0.5
-1.0

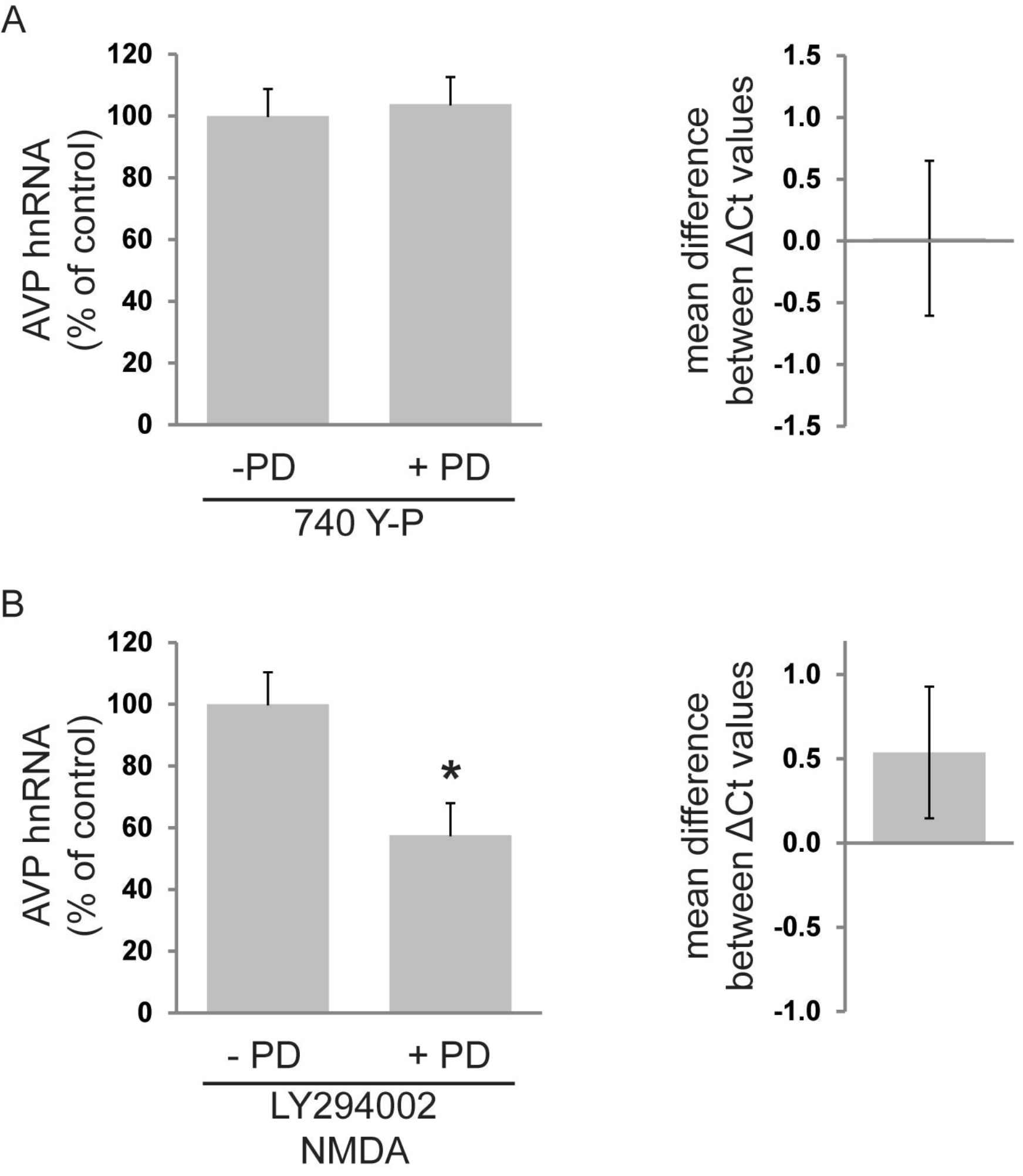
A
AVP hnRNA
(% of control)
120
100
80
60
40
20
0
-PD
+ PD
740 Y-P
mean difference
between ΔCt values
1.5
1.0
0.5
0.0
-0.5
-1.0
-1.5
B
AVP hnRNA
(% of control)
120
100
80
60
40
20
0
*
- PD
+ PD
LY294002
NMDA
mean difference
between ΔCt values
1.0
0.5
0.0
-0.5
-1.0